DOI 10.1007/s11182-023-02996-z

Russian Physics Journal, Vol. 66, No. 6, October, 2023

INTERACTION OF SATELLITE NAVIGATION SIGNALS WITH FOREST AND SNOW-ICE LAYERS

M. Yu. Reushev,[1,2] V. G. Podoprigora,[2,3] D. S. Makarov,[1,5] D. V. Kharlamov,[1] and E. V. Vasiliev[4]

UDC 537.86

The paper studies parameters of the snow-ice cover and forest ground determined by the integrated approach based on the global navigation satellite system reflectometry. Experimental data on the amplitude and time response of satellite navigation signals are processed by fast Fourier transform and then analyzed using mathematical methods based on the multipath echoes model in terms of geometrical optics. Using a combination of reflectometry and numerical simulation of the surface layers based on local weather data, it is possible to evaluate not only the current state of these layers, but also predict their dynamic development.

Keywords: global navigation satellite system reflectometry, navigation signal, interference, multipath echoes, surface layers.

INTRODUCTION

L1 and L2 signals in the global navigation satellite system (GNSS) frequency band, provide the space-time data acquisition of electromagnetic wave scattering, signal reflection/absorption in air and on the ground [1, 2]. Signal changes are caused by various electrophysical parameters of media. The global navigation satellite system reflectometry (GNSS-R) is the most popular method of studying such changes. The GNSS-R can restore significant media parameters, namely: the layer thickness and density, signal attenuation and scattering, humidity, topographic ruggedness, etc.

Multipath interference is reflected in the fact that additional frequencies appear along with the fundamental frequency matching the reflection from the surface. These frequencies are provided by the propagation of some navigation signals in the snow-ice cover. Additional frequencies occur after recording the amplitude and time response of signals and their successive processing by fast Fourier transform (FFT). The reflection from the snow-ice cover is mirror reflection, since the root-mean-square (RMS) deviation of the ruggedness is significantly lower than the signal wavelength. This does not lead to the diffraction scattering causing a phase fluctuation of the reflected signal.

MULTIPATH INTERFERENCE IN GNSS

Figure 1 schematically illustrates the multipath interference in navigation signals reflecting from the snow/ice/water layer [3, 4]. In addition to the reflection from the forest ground, the navigation signal may consist of the

[1]Krasnoyarsk Research Center of the Siberian Branch of the Russian Academy of Sciences, Krasnoyarsk, Russia, email: reuqem@mail.ru; mcdan3991@yandex.ru; dimafeadz@gmail.com; [2]Siberian Federal University, Krasnoyarsk, Russia, email: podoprigora46@gmail.com; [3]Kirensky Institute of Physics of the Siberian Branch of the Russian Academy of Sciences, Krasnoyarsk, Russia; [4]Institute of Computational Modeling of the Siberian Branch of the Russian Academy of Sciences, Krasnoyarsk, Russia, email: ven@icm.krasn.ru; [5]Reshetnev Siberian State University of Science and Technology, Krasnoyarsk, Russia. Original article submitted August 24, 2023.

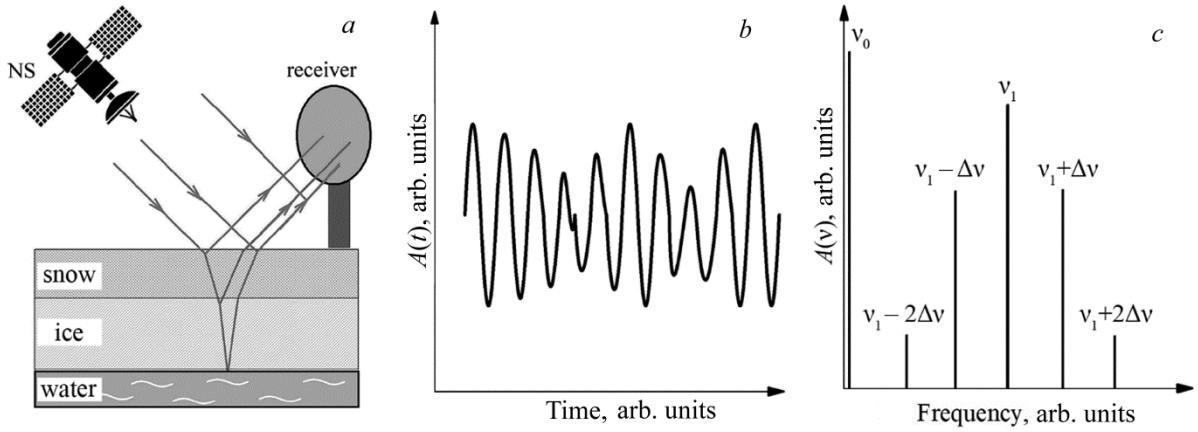

Fig. 1. Schematic of multipath interference in snow-ice cover: *a* – reflectometry; *b* – amplitude and time response of navigation signal; *c* – FFT analysis of amplitude and time response.

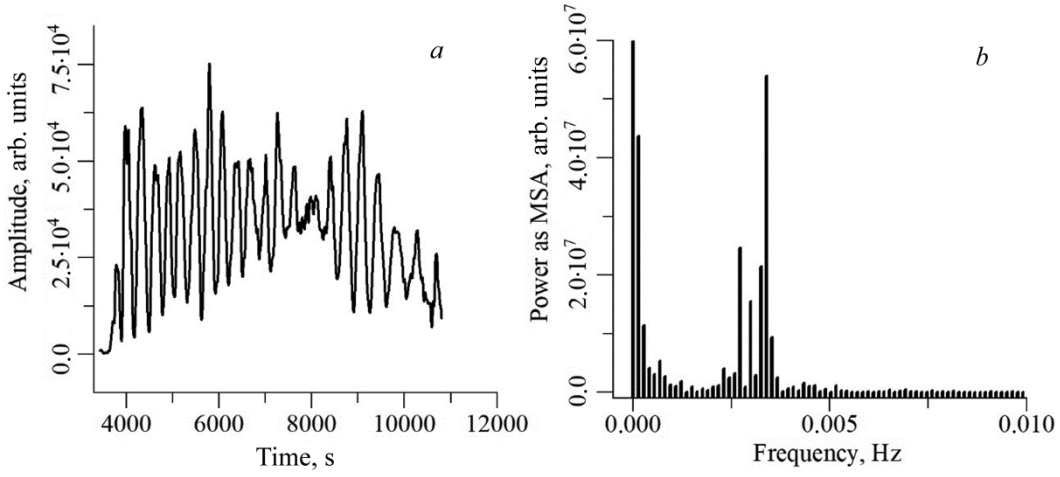

Fig. 2. Traces of navigation signals reflected from the ice sheet: *a* – amplitude and time response, *b* – FFT.

diffraction component provided by scattering over large-scale forest ruggedness and multipath radiation scattering in tree crowns and their mutual interference.

When the forest ground roughness is lower than the signal wavelength, the incoherent component is much less than the coherent. The signal attenuation grows and coherent scattering reduces with increasing density of the forest stand. For comparison, Figs. 2 and 3 show the results of FFT-based processing of the amplitude and time response of navigation signals received by GNSS with right-hand circularly polarized signals and the data refresh rate of 1 Hz.

Reflectometry results presented in Fig. 2, describe signals reflected from the ice layer 40 cm thick. A standard procedure [4] is used to measure the amplitude and time response of signals near Lake Bugach (Krasnoyarsk region) in winter 2022–2023. Figure 3 presents traces of continuous electromagnetic transmission probing of a pine forest near the Krasnoyarsk Research Center SB RAS in summer 2022.

As can be seen in Fig. 2, in addition to the fundamental frequency in the trace spectrum, there are unwanted frequencies generated by the electromagnetic emission signals of the navigation system penetrating into the ice sheet, reflection from the medium boundaries, and in-plane reflected beam interference of the receiving antenna.

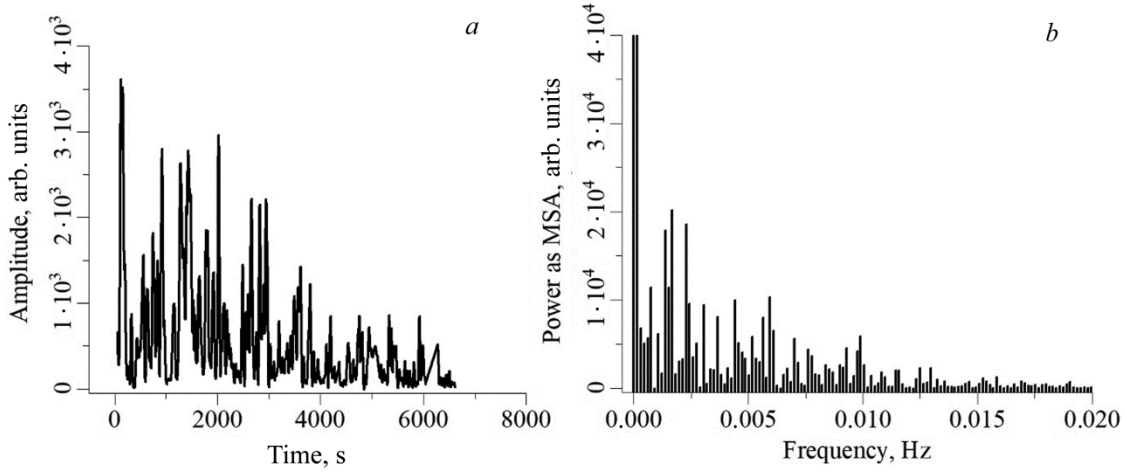

Fig. 3. Traces of continuous electromagnetic transmission probing of the forest: *a* – amplitude and time response, *b* – FFT.

In Fig. 3, one can clearly see the spectral diffusion component nearby the fundamental frequency. This is because the primary signal interference of the navigation system and its reflection from the forest ground. The diffusion component envelope is described by the following relation:

$$S(\nu) = S_0 \exp(-\alpha\nu + \beta) + C ,$$

where S_0 is the maximum value of $S(\nu)$ function; α, β and C are function indicators depending on the signal absorption by the forest.

Further experiments showed that identification of α and β coefficients determined by the GNSS-R, can be used to control the forest quality provided that these coefficients refer to the forest stand structure. Such a reference is possible only in creating the experimentation facility during multiple measurements.

In terms of geometrical optics, the multipath echoes model is used to describe the GNSS-R results of ice and forest and calculate parameters of reflected signals and those passed through the layers. According to the similar model proposed by Ulaby *et al*. [5], the structure consists of the air layer and localized parallel layers of snow, ice, and freshwater. According to [5], permittivity ε for the snow layer 10 cm thick with vertically averaged density is $1.389 - i \cdot 2 \cdot 10^{-4}$; for 44 cm thick ice layer it is $2.93 - i \cdot 8 \cdot 10^{-4}$, and for the water layer it is $82 - i \cdot 2.5$. Satellite navigation signals reflected from the layers (L1 ≈ 19 cm), are coherent (~1 s coherence time). As a result, the RM deviation σ of the ruggedness from the average snow-ice cover is on the order of ≈1 cm [5]; the reflection from the snow-ice cover is mirror reflection.

The amplitude U_i of the signal wave reflected from the i-th layer, can be described by the following relation [2]:

$$U_i = R_{i,i+1} \prod_{k=1}^{k=i} T_{k-1,k} T_{k,k-1} e^{-2\alpha_k d_k} ,$$

where T_{ij} and R_{ij} are transmission and reflection coefficients of the i-th and j-th layers, respectively; $\alpha_k = 2\pi\lambda^{-1} \times |\mathrm{Im}(\sqrt{\varepsilon_k})|$ is the attenuation coefficient in the k-th layer; $d_k = H_k/\cos(\theta_k)$, where H_k and θ_k, are the thickness and angle of incidence in the k-th layer, respectively. In this case, the beam propagation in a multilayer plate follows Snell's law:

$$\sqrt{\varepsilon_{k-1}} \sin\theta_{k-1} = \sqrt{\varepsilon_k} \sin\theta_k .$$

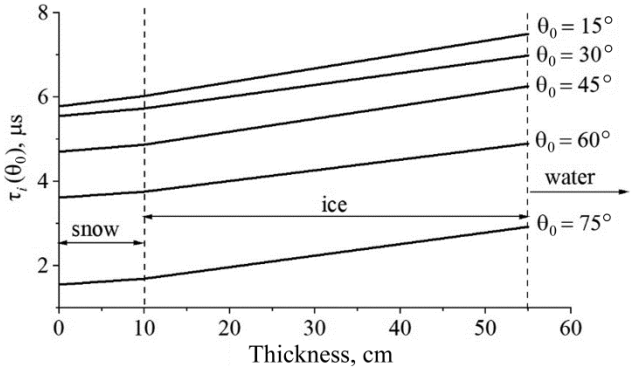

Fig. 4. Dependences between the time delay τ_i and snow-ice cover thickness at different angles of incidence θ_0.

The signal delay τ_i during which the beam falls onto the snow layer and propagates toward the *i*-th layer, reflects from it and reaches the receiver, which is described by the equation

$$\tau_i = \tau_0 + \sum_{k=1}^{k=i} 2n_k \cdot d_k - \left(\sum_{k=1}^{k=i} D_k \right) \cdot \sin\theta_0 ,$$

where $\tau_0 = 2H_0 \cdot \cos(\theta_0)$ is the time delay between the mirror reflection from the upper air/snow interface and the main beam; $n_k = \sqrt{\varepsilon_k}$ is the refractive index of the *k*-th layer; $D_k = 2H_k \cdot \tan(\theta_0)$.

Figure 4 presents dependences between the time delay and snow-ice cover thickness at different angles of incidence.

The time delay generates the phase specified by the relation $\varphi_i = 2\pi\ \tau_i/\lambda$. The navigation signal received by the antenna, is the total sum of the modulated primary signal and superposition of signals reflected from each layer. Varying the incident angle, it is possible to change not only the amplitude, but also phases of reflected waves. The waveform distortion is insignificant due to the mirror reflection from smooth surfaces.

Specific properties of GNSS signals propagating in the medium, are determined by their high stability and sensitivity to the layer structure, that allows using them in radiography to observe layers of different thickness based on the frequency of signal interference. `

ICE SHEET DYNAMICS MODELING

Since the GNSS-R is aimed at the parameter determination of the ground layers such as ice, snow, water, and stand forest, the dynamic development of these parameters is of great importance. For example, information about the temperature and ice sheet conditions can be obtained from numerical simulation based on local weather data. Numerical simulation allows evaluating not only the current state of the ice sheet, but also predict its future dynamics based on meteorological forecasts.

Ice-sheet dynamics modeling is based on the numerical solution of the Stefan problem. The problem is presented in a generalized formulation, when the heat of the ice-water phase transition is considered in the effective heat capacity of the medium [6, 7]:

$$c_S(z)\rho(z)\frac{\partial T}{\partial t} = \frac{\partial}{\partial t}\left[\Lambda(z)\frac{\partial T}{\partial z}\right] + q_V(z),$$

where c_s, ρ are effective heat capacity and density of the medium; T is the temperature; Λ is thermal conductivity; t is the time; z is the vertical coordinate directed downwards from the surface, q_v is the power of the volume heat source

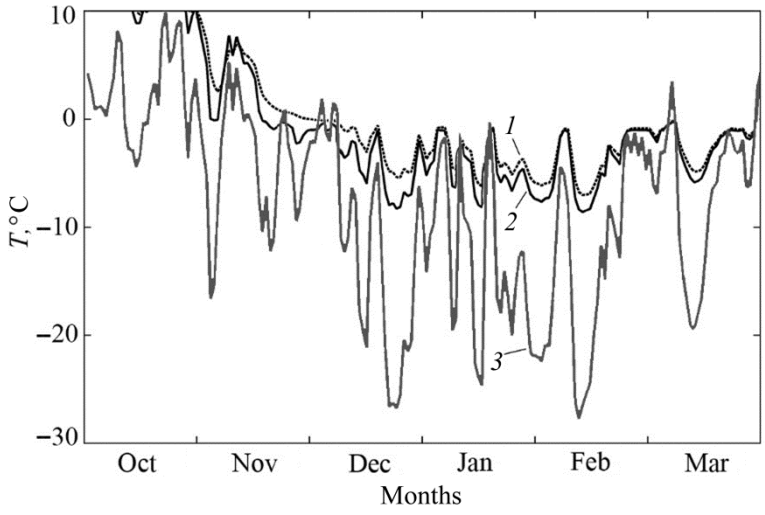

Fig. 5. Time dependences of temperature in the ice sheet layers.

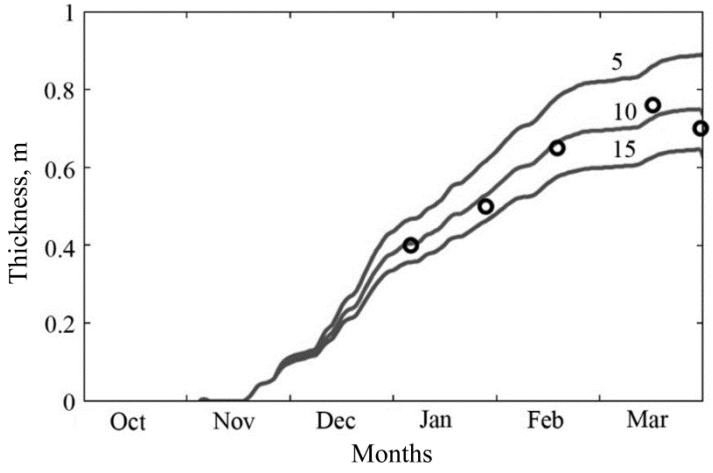

Fig. 6. Time dependences of ice thickness $d(t)$.

determined by the absorption of the solar radiation flux deep in the layer. Heterogeneities of c_s, ρ and Λ are associated with the presence of the phase change and the difference in physical properties of water, ice and snow. The heat transfer equation is supplemented by a third-order boundary condition at the upper boundary of reservoir [6]:

$$\left[\frac{\partial T}{\partial z} + T\right]_{z=0} = q\big|_{z=0} \cdot$$

This boundary condition allows considering the heat transfer in the surrounding air using the coefficient α_T including heat flows produced by the reservoir radiation, atmospheric thermal radiation, and evaporation. The calculation procedure for heat flows is described in [8]. These calculations utilize the cold period climatic data (October 2021 till March 2022) gathered by the Minino weather station (latitude: 56.07, longitude: 92.73) situated near Lake Bugach.

In Fig. 5, one can see the time dependences of the air temperature (curve *1*), ice sheet (curve *2*), and ice sheet 10 cm thick (curve *3*) with the snow layer 10 cm thick [7].

The ice thickness $d(t)$ can be calculated using the temperature dependences. This is presented in Fig. 6. Circles indicate the ice thickness obtained by direct measurements of the ice sheet on Lake Bugach.

CONCLUSIONS

Based on a combination of GNSS-R of the ground layers and numerical simulation, information about the structural properties is obtained continuously and promptly. This information can be readily used in forestry, by the Emergencies Ministry, and in other economic activities of the Russian Federation.

REFERENCES

1. V. B. Kashkin, T. V. Rubleva, K. V. Simonov, *et al*., Applied Aspects of Geosphere Research Using Satellite Technologies [in Russian], Krasnoyarsk (2023). ISBN 978-5-7638-4704-8.
2. S. Jin, E. Cardellach, and F. Xie GNSS Remote Sensing, Springer Dordrecht Heidelberg, New York; London (2014).
3. M. I. Mikhailov, A. V. Sorokin, and V. L. Mironov, Izv. Vyssh. Uchebn. Zaved., Fiz., **58**, No. 10/3, 70–72 (2015).
4. D. S. Makarov, D. V. Kharlamov, and A.V. Sorokin, Sibirskii zhurnal nauki i tekhnologii, **20**, No. 1, 8–19 (2019).
5. F. Ulaby, R. Moore, and A. Fung, Microwave Remote Sensing Active and Passive, I–III: Artech House (1990).
6. E. N. Vasiliev, D. S. Makarov, and A. V. Sorokin, Tekhnika i tekhnologiya, **15**, No. 2, 261–271 (2022).
7. E. N. Vasiliev and V. A. Derevyanko, Thermophysics and Aeromechanics, **25**, No. 3, 461–467 (2018).
8. E. N. Vasiliev, J. Sib. Fed. Univ. Math. Phys., **15**, No. 6, 753–762 (2022).